Original Imaging Technologies

rimtech

EqueTom™

Portable tomosynthesis system for equine market

User Manual

Tomosynthesis Image Quality and Case Studies

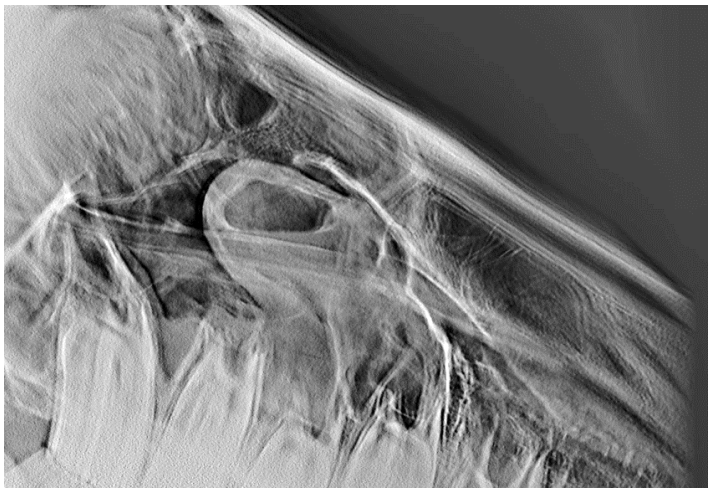

Hotline

Request additional information from:

Orimtech LTD.

1611 Barclay Blvd,

Buffalo Grove, IL 60089

USA

+1 847 250-2121

Copyright

Document Version

Orimtech reserves the right to change its products and services at any time.

The reproduction and distribution in any form are strictly prohibited without prior authorization from Orimtech LTD.

The information in this documentation is subject to modifications without notice.

Disclaimer

Orimtech provides this documentation "as is" without the assumption of any liability under any theory of law.

This manual is only intended for the owners of EqueTom™ equipment and their staff.

Content

Introduction

The **EqueTom™ User Manual – Tomosynthesis Image Quality and Case Studies** presents a part of the instructions required for safe and correct device use.

The following manuals, supplied with the device for user consultation, are an integral part of the instructions required for use of the **EqueTom™** system:

- **EqueTom™ User Manual**;
- **EqueTom™ Quick Start Guide**.

The **EqueTom™ User Manual – Tomosynthesis Image Quality and Case Studies** contains a description of the tomosynthesis image forming principles, measurements, technical specifications, as well as clinical cases samples helping for learning images analysis basic principles.

1 Image Quality in Tomosynthesis

1.1 Digital Tomosynthesis method description

X-ray digital tomosynthesis (DT) is a new method of examination in veterinary medicine. In terms of the simplicity of performing examinations, DT is close to digital radiography (DR), and in terms of efficiency, it is close to computed tomography (CT). The development of X-ray examination methods leads to an increase in the number of measured parameters of diagnostic images. DT provides new opportunities for both observation and measurement of image parameters of layers.

EqueTom™ (ET) tomosynthesis system for equine market is the world's first diagnostic mobile x-ray unit for examining horses using digital tomosynthesis method. It implements the principle - not bring a horse to CT, but bring CT to the horse (**Figure 1**).

During the examining, the horse is calmly standing on a dry hard surface, and the operator places the ET device in the desired position (**Figure 1b, c**).

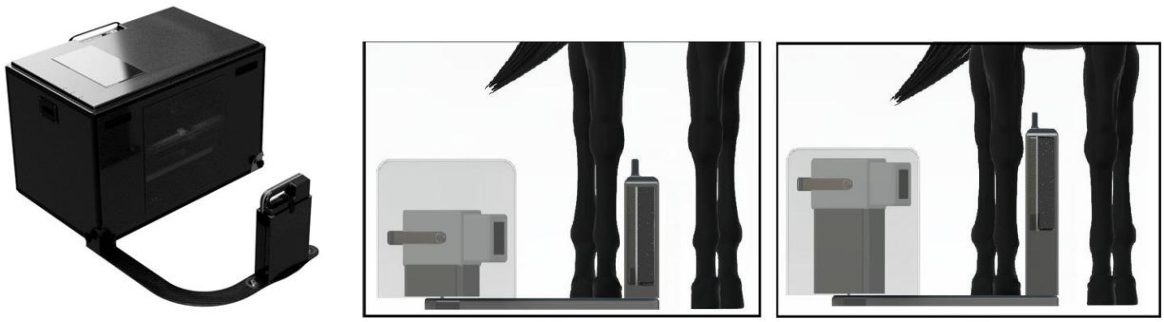

a) b) c)

Figure 1. Appearance – **(a),** positioning ET – **(b)** and **(c).**

During scan procedure X-ray generator moves inside the ET gantry within 2.5 ... 3.2 s. During the scan time, a dynamic digital X-ray receiver (DDR) generates 85 ... 120 X-ray images (projections) of the examined part of a horse, taken at different angles. Acquired X-ray images are transmitted to the computer. Then tomographic reconstruction and mapping of 150 ... 340 X-ray layers parallel to the plane of the detector are performed.

The following describes the basics of the work of a veterinarian in observing images of tomographic layers and measuring their parameters. The features of the implementation used in digital radiography and computed tomography measurements. Additional features of tomosynthesis are shown when measuring small structures in the images of layers. Such measurements are particularly useful in analyzing the state of the trabecular (spongy) and cortical (hard) parts of the bone.

1.2 Cross-sectional images in tomosynthesis

In appearance, the images of the layers in the system with tomosynthesis (DT) differ from digital X-ray images (DR) and CT images **(Figure 2).** Doctor viewing of DT - images is similar to viewing optical images using a microscope or binoculars. In these cases, focusing on depth is implemented. On the DT - image, there is a sharp X-ray image of the layer at a certain depth and weakened, de-focused images of the adjacent layers.

DR

CT

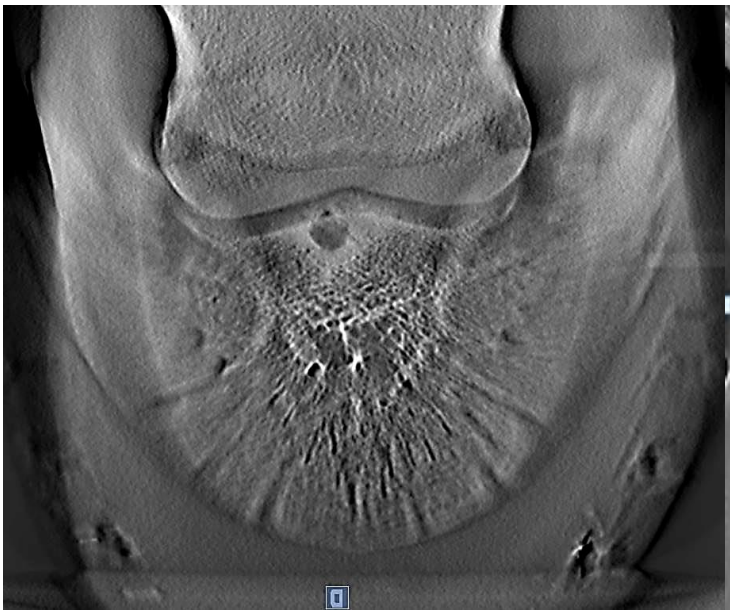

DT

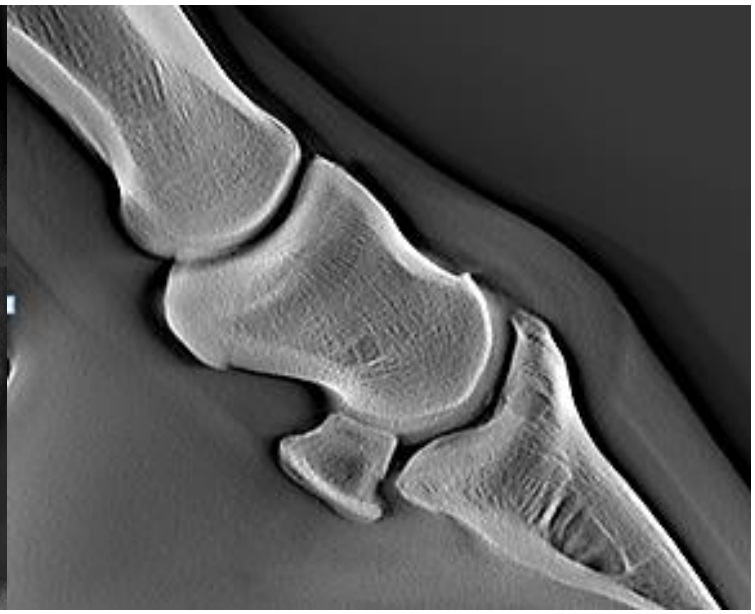

DT

Figure 2. Sample images obtained on DR, CT and DT systems.

The presence of de-focused adjacent layers on the DT image allows the operator to easily navigate the depth of the examined object. Similarly, the vision of a person in the daily life. Therefore, a sequence of DT images of layers is more familiar than a sequence of CT slices. In addition, DT images from the EqueTom™ tomosynthesis system have approximately twice as much detail as compared to images of conventional CT scanners.

Analysis of DT image layers diagnostic sequence has great advantages compared with the analysis of DR images.

On the DR images, all layers of the object of examination are superimposed on the image in the plane of the receiver with different geometrical magnifications **(Figure3).**

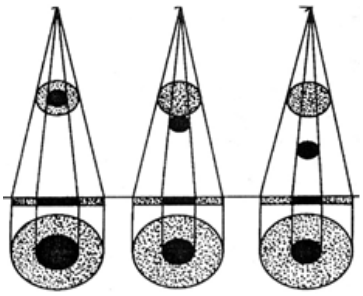

Figure 3. Imposition and geometric magnification inspection of objects on x-ray radiography image.

There are measurement errors and ambiguity of image analysis. To partially mitigate this effect several X-ray pictures are usually taken at different angles (for example frontal and lateral X-ray images **(Figure 4)**).

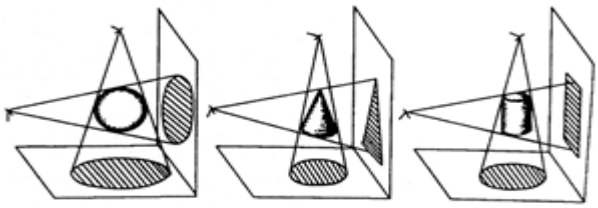

Figure 4. The sets of frontal and lateral X-ray radiography images.

Analysis of the aggregation of DR images does not eliminate measurement errors, but makes the analysis more unambiguous.

Further development of this approach is implemented in tomosynthesis systems. The sequence of 80...110 X-ray images of a dynamic digital receiver (DDR) in the EqueTom™ tomosynthesis system is performed at the corners (**Figure 5, a**) of scanning up to ±12º.

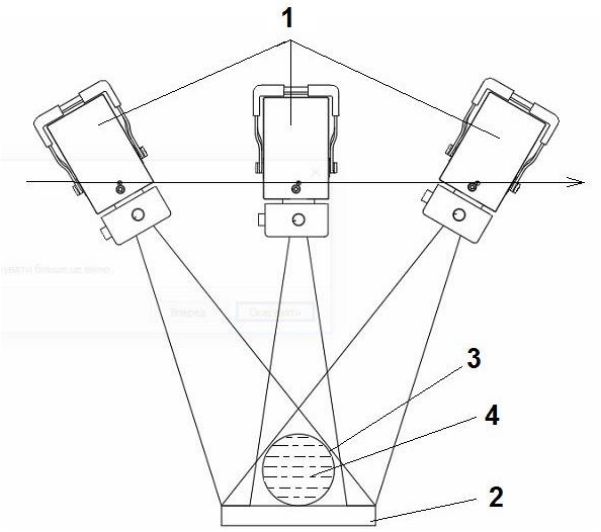

a)

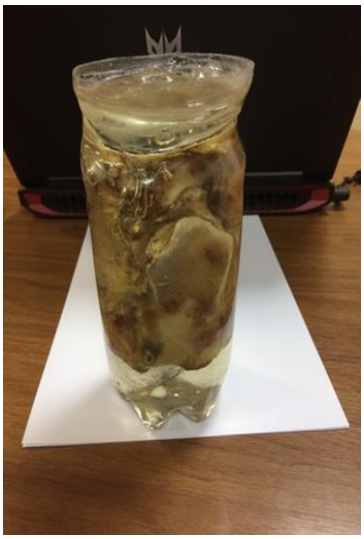

b)

Figure 5. Scanning principle (a): generator -1, DDR -2, object of examination by EqueTom™ tomosynthesis system - 3, position of the tomosynthesis layers of the object - 4. Photo of the phantom (b).

The doctor may look at the original X-ray images of DDR, but it is much more convenient to analyze the images after tomographic reconstruction. The presence of tomosynthesis layers allows to:

- observe the object of examination in the form of a sequence of layers images of sections, focused at different depths;
- observe the details of an object with a contrast several times greater than the contrast of the details of an object on an X-ray image;
- measure the spatial dimensions of objects without geometric magnification errors;
- measure the depth of the part of the object by the layer number;
- assess the X-ray density of the object in the layer, taking into account the influence of the weakened defocused images of adjacent layers;
- measure the intensity of small structures in the layer.

It is convenient to illustrate the noted possibilities by the example of images of the phantom limb join of a large animal. Such a phantom **(Figure 5, b)** contains real bones and cartilages of the joint, as well as added test objects that imitate various types of pathologies encountered in injuries and diseases of the joints of horses' limbs.

When observing and measuring, the user interface is used **(Figure 6),** in which there are main windows: “Database”, “Radiography” and “Tomography”. These windows determine the main modes of user operation: patient selection and images for diagnosis, analysis of x-ray images and analysis of the results of tomosynthesis.

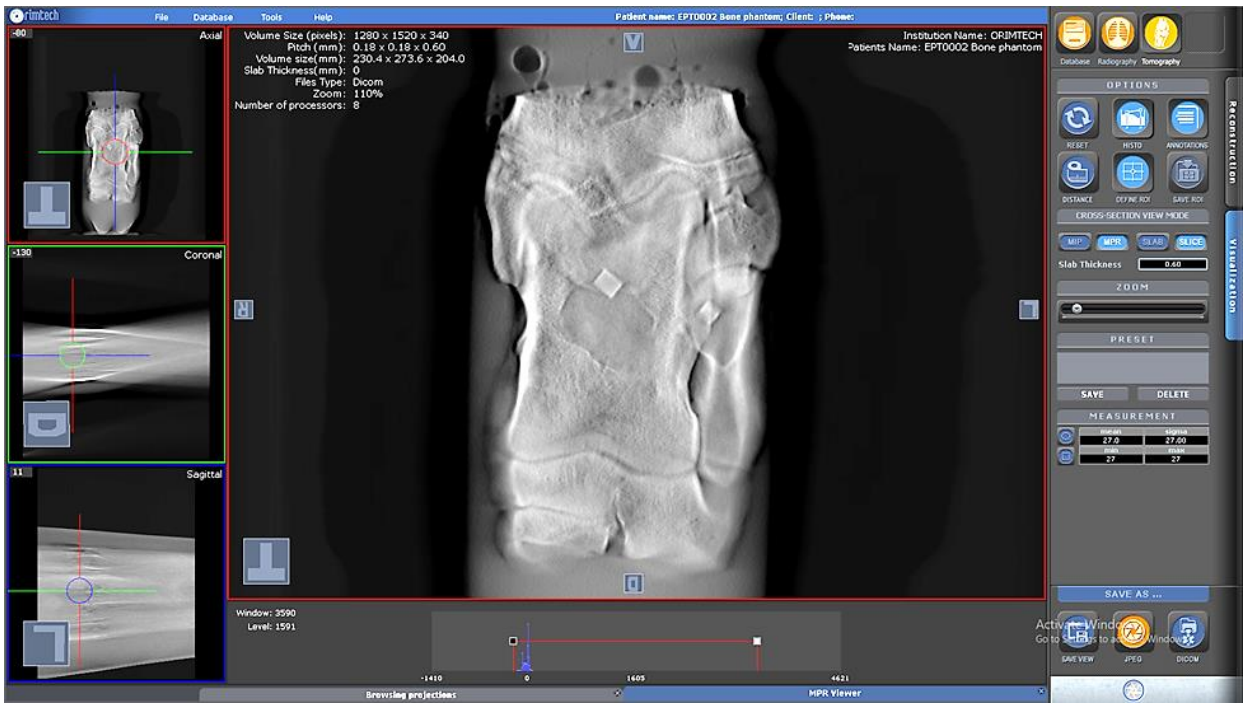

Figure 6. User interface in “Tomography” mode.

The “Tomography” mode shown in **Figure 6** is essential for further discussion.

1.3 Spatial resolution of the EqueTom

The spatial resolution of the x-ray image is measured in the lines pairs per millimeter (lp/mm). This is similar to traditionally used in optic measurements of the number of the optical ruler strokes per millimeter, visually observed at the output of an optical device. The X-ray rulers are used to measure the spatial resolution of the x-ray image. Ruler consists of two layers of plastic, between which there is a layer of lead 50 ... 60 microns thick, having a certain pattern. Typically, the drawing contains wedge-shaped strips with a scale of their spatial density **(Figure 7, a)** or a group of 3

strokes with different spatial density **(Figure 7, b).** The high contrast of the x-ray image of the ruler allows you to visually determine the ability of the x-ray system to show fine examination object details.

a) b)

Figure7. X-ray rulers for spatial resolution measurement.

In practice, the measurement of resolution consists in the visual assessment of the limit of observability on the X-ray image of the most densely located strokes and the reading of the values of spatial density on the word scale.

The highest resolution has radiographic systems. For most flat panels, the spatial resolution is 3.7...4.0 lp/mm. In the graphical mode, the ET receiver has a higher spatial resolution - about 5.0 lp/mm.

In tomosynthesis mode, the spatial resolution of **the EqueTom™** has a maximum value in the 10 cm zone near the receiver input window - about 2.2 lp / mm. The farther we set the examination object from the input window of the receiver, the lower resolution we get. At a distance of 15 ... 20 cm from the terminal, the spatial resolution of the ET will be 1.8 ... 2.0 lp / mm. For comparison, usually the spatial resolution of the CT is about 1.0 lp / mm, i.e. 2 times less than the ET.

1.4 Resolution in depth (Layer Thickness), in depth measurements.

Scanning by an x-ray generator in tomosynthesis mode allows to observe objects from different angles and focus on depth. The larger the scanning angle, the more precise the depth of the objects can be determined. The entire volume of the analyzed space is divided into separate layers in depth. In each layer, the image contains a focused image of this layer and de-focused and weakened images of adjacent layers. The larger the scanning angle, the thinner the layers can be reconstructed.

On the other hand, if two objects are coaxially located on the adjacent layers in the direction of X-rays, then X-ray imaging will superimpose their images. During tomosynthesis, due to observation at angles and a different location in depth, these objects can be observed separately.

The thickness of the tomosynthesis layer is the minimum depth distance at which objects of one pixel in size can be observed separately at a given scan angle **(Figure 8).**

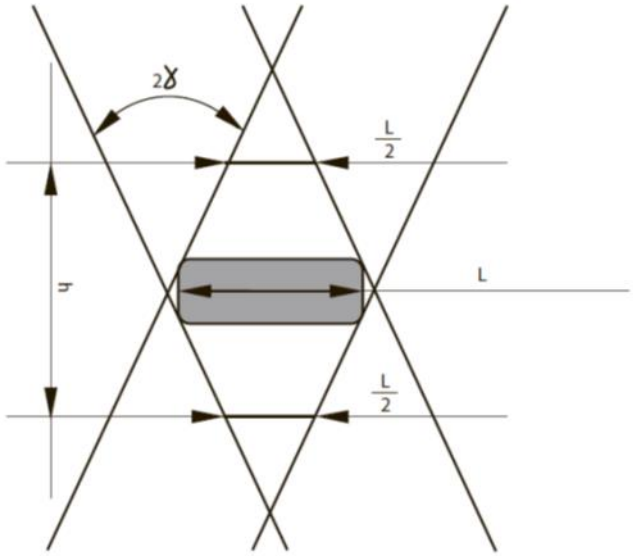

Figure 8.Calculation of the slice thickness in the tomosynthesis mode. Gray rectangle denotes the planar reconstructed object. L- is size of the object in tomosynthesis plane, 2 γ- is angular scan range, h- is the slice thickness.

From the simple geometrical considerations we derive the following relation for the slice thickness h:

$$h = \frac{L}{2\ tg\ \gamma}.$$

For example, with the resolution of ET X-ray images at 2.2 lp/mm, the pixel size will be

*L = 1/2*2,2 = 0,23 mm.*

If you use a scan angle of 2 γ = 20^{O}, layer thickness

h = L/tg γ = 0,23/2 tg 10^{O} = 0,65 mm.

At a smaller scanning angle 2 γ = 11^{O}, layer thickness

h = L/tg γ = 0,23/2 tg 5.5^{O} = 1,19 mm.

In **EqueTom™** unit, the scan angle usually does not exceed 20 °, therefore during reconstruction the tomosynthesis layers are calculated through 0.6 mm.

When analyzing tomograms, the layer number is displayed on the monitor in the upper left corner **(Figure9).**

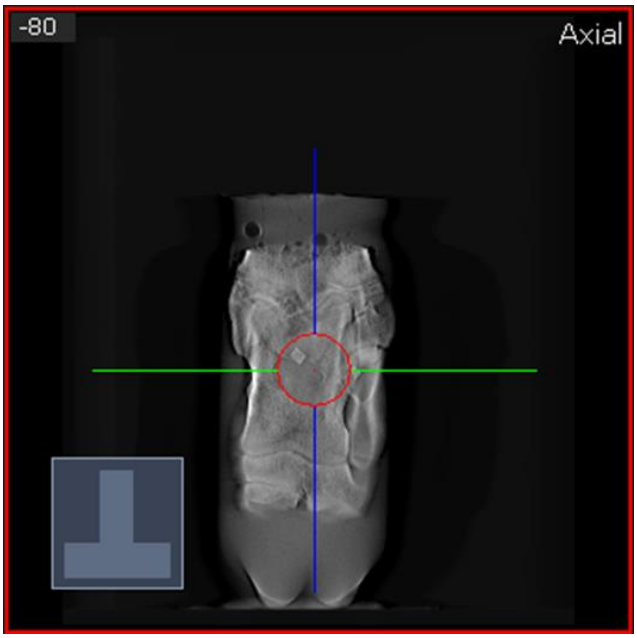

Figure 9.Upper left corner location of the layer number on the monitor screen.

Information about the selected step of tomogram layers is contained **(Figure6)** in the image description, where the entry "Pitch: 0.2x0.2x0.6" means the dimensions of the tomogram voxel — 0.2 mm by 0.2 mm in terms of image and 0.6 mm - voxel size in depth or - layer spacing.

To measure the position of the object in the depth H_O, the N_O layer number should be multiplied by the layer thickness h:

$$H_O = N_O * h,$$

and to measure the thickness of the object is to find the difference

$$\Delta H = H_{O1} - H_{O2},$$

where - H_{O1} and H_{O2} - the depth of the beginning and the end of the object layers

The thinner the layer, the more accurately you can measure the depth of the observed object and its thickness.

To illustrate the depth measurement capabilities, as an object of observation, we will select a test object in the form of a rectangular bone plate with a size in the 6x5mm in the plane of the phantom **(Figure6)** and a depth of 3.2mm.

The initial and final layers of the image will be determined by the appearance on the image of the hard edges of the plate bone. Because of measurements for the scanning angles of 11^O, 15^O and 20^O, values of 10.2 mm, 4.8 mm and 3.6 mm can be obtained.

Obviously, the highest measurement accuracy corresponds to the widest scan angle of 20^O. The magnitude of the resulting discrepancy between the measured and the actual thickness of the bone plate was 0.6 mm, which satisfy any task of veterinary diagnostics.

1.5 Cross-sectional observation of a limb joint phantom.

Layered observation is performed at the first stage of the survey. At this stage, the doctor analyzes the general condition of the solid and spongy parts of the bones of the animal. To demonstrate the benefits of tomosynthesis in Figure 10, a, b positive and negative x-ray images are shown, and in Figure 11, a-f shown the phantom layers selected for analysis.

.

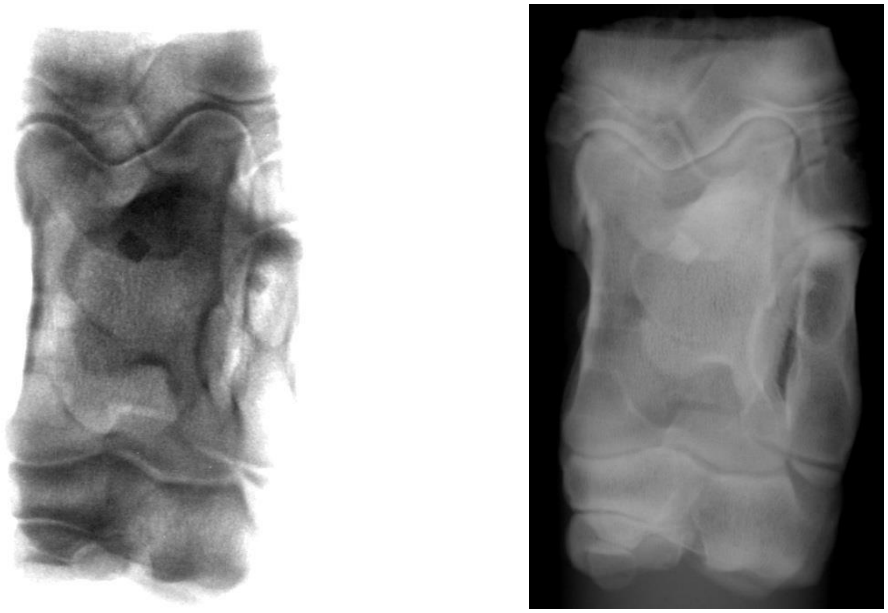

a) b)

Figure 10. Positive - (a) and negative - (b) X-ray images of a phantom.

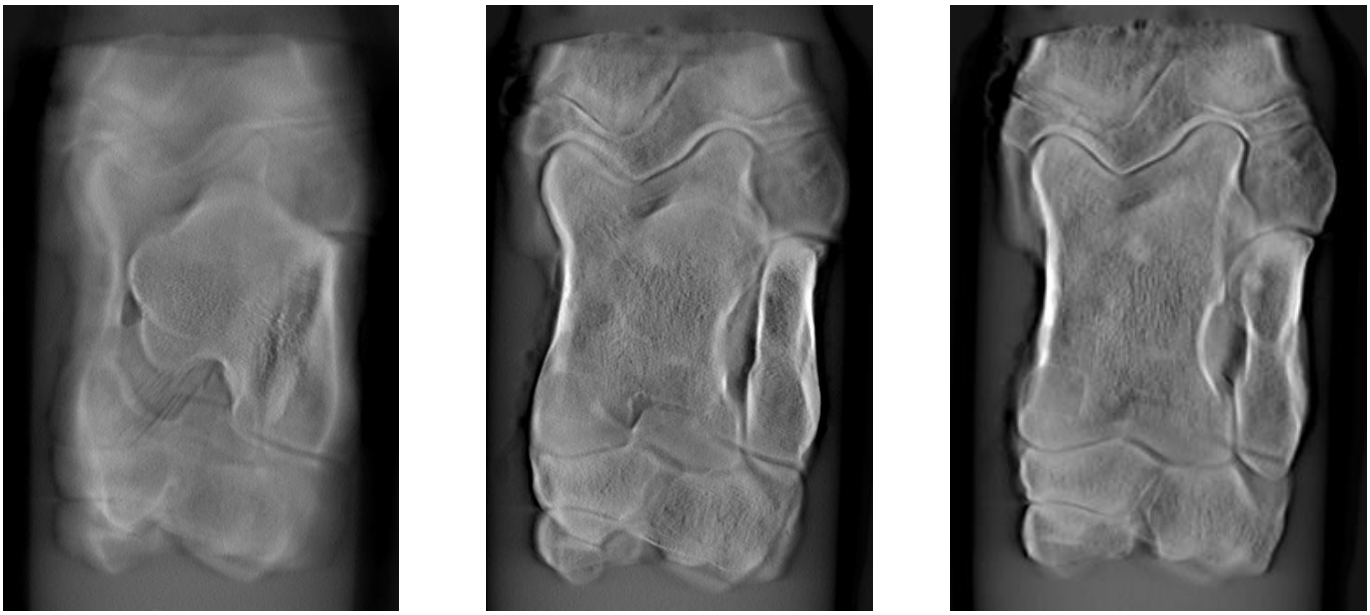

a) b) c)

d) e) f)

Figure 11. Phantom layers: 10th - (a); 40th - (b); 60th - (c); 70th - (d); 80th - (e); 90th – (f).

Layer-by-layer observation of the phantom joint (Figure 11, a - f), by increasing the layer number, the following features can be distinguished:

Layer 10. The layer occupies only the central part of the image of **Figure 11 a**, where small details are clearly visible. Above and below layer 10 in the image there is a defocused image of subsequent layers, giving an overview of the phantom. On display of the layer 10 is clearly visible small-sized structure of a trabecular bone (**Figure 11 a**); at the bottom left of the image, there are clear low-contrast bands imitating vessels. On the X-ray image (**Figure10 a, b**) the fine structure is distorted, the “vessels” are not visible.

Layer 40. The large structure of the trabecular bone is clearly visible in the image (**Figure 11 b**). On the X-ray image (**Figure 10 a, b**), the large structure of the trabecular bone is obscured by a non-uniform background.

Layer 60. In the center, to the left of the image, areas with the absence of trabecular bone are clearly visible (**Figure 11 c**). On the phantom, they are formed by drilling holes in a bone with a diameter of 10 mm, 5 mm and 3 mm to a depth of about 15 mm. On the x-ray image (**Figure10 a, b**) areas with the absence of trabecular bone are seen as more transparent formations.

Layer 70. In the center and on the right in the image, two contrasting rectangular objects with a cortical bone density are visible (**Figure 11 d**). In phantom for simulating bone fragments and bone pathologies test objects set of rectangular cortical bone size 6x5 mm 4,5x3,5 mm and thickness 4.0 and 4.5 mm. On the x-ray image (**Figure10 a, b**), rectangular objects are visible as low contrast bone formations.

Layer 80. In the center of the image below two rectangular objects, an area with no bone structure is visible (**Figure 11 e**). On the phantom is a recess due to the structure of the joint in normal anatomy. On the X-ray image (**Figure 10 a, b**) the incision is masked by other bone formations.

Layer 90. In the center, to the left of the image, there is a third contrasting triangular object with a solid bone density (**Figure 11 f**) in addition to two contrasting rectangular objects. On the phantom, it is formed by installing a test object of a triangular shape made of solid bone with a base size of 4.5 mm, a height of 5.5 mm and a thickness of 4 mm. On the X-ray image (**Figure 10 a, b**), the object of a triangular shape has low contrast and is masked by other bone formations.

The number of the tomosynthesis image layer depends on the depth of the object of analysis and the layers selected by the operator during the reconstruction of the reference point and the pitch between the layers. In the example shown in Figure11, a-f, the zero layer corresponds to the front edge of the phantom, and the distance between the layers during the reconstruction is set to h = 0.6 mm. Thus, the 10th layer, shown in Figure11 a is located at a distance:

$$Z_{10} = 10^* h = 10^*0,6 = 6 \text{ mm}$$

from the front edge of the phantom. The last of the layers in Figure 11 at number 90 is located at a distance:

$$Z_{90} = 90^* h = 90^*0,6 = 54 \text{ mm}$$

from the front edge of the phantom. The distance between the 10th and 90th layers is 80 layer pitch or 48 mm. This value is confirmed by direct measurement of the phantom.

1.6 Observation of destruction and anomalies of cortical bone, contrast measurements.

After layer-by-layer observation of the zone of interest, the destruction and anomalies of the cortical bone are often observed. The high contrast of the formations of interest increases the effectiveness of such an observation.

The use of a phantom makes it possible to compare the contrast of the image details in the tomographic layer obtained on the EqueTom™ tomosynthesis system with the contrast of the details of the object on radiographic X-ray images.

Initially, we measure the brightness of test objects simulation bone fragments (**Figure 10,b**) on radiographic X-ray image with the parameters Ua = 75 kV, Q = 5 mAs. Contrast is computed according to the formula:

$$K_{DR} = (B_O - B_{bg})/B_{bg},$$

where B_O – average brightness of the test object (in units of grayscale - GS);

B_{bg} - average background brightness near the test object;

K_{DR} – contrast of an object in a DR x-ray image.

Table 1.The results of measurements on the x-ray image.

Object	Triangular 4,5x5,5 mm	Rectangular 6x5mm	Rectangular 4,5x3,5 mm
B_O, GS	5923	5057	6044
B_{bg}, GS	6169	5152	6274
K_{DR}, %	4,0	1,8	3,7

Thus, the measured contrast of test objects that simulate bone fragments on a x-ray image with the parameters Ua = 75 kV, Q = 5 mAs, was 4.0%, 1.8% and 3.7% (Table 1).

Then, similarly, we measure the brightness of the same test objects on the images (Figure11 d-f) of tomographic K_{DT} layers with the tomosynthesis parameters Ua = 75 kV, Q = 50 mAs. Contrast is computed according to the formula:

$$K_{DT} = (B_{OT} - B_{bgT})/ B_{bgT},$$

where B_{OT} – tomosynthesis average brightness of the test object (in units of grayscale - GS);

B_{bgT} – tomosynthesis average background brightness near the test object (Table2).

Table 2. The results of measurements on the x-ray image.

Object	Triangular 4,5x5,5 mm	Rectangular 6x5mm	Rectangular 4,5x3,5 mm
B_{OT}, GS	2122	1723	1844
B_{bgT}, GS	1560	1496	1508
K_{DT}, %	36	15	22

According to the results, the measured contrast of test objects imitating bone fragments in tomographic images with tomosynthesis parameters Ua = 75 kV, Q = 50 mAs was 36%, 15% and 22%.

An increase in the contrast of test objects imitating bone fragments on x-ray phantom images during the transition from X-ray to tomosynthesis is equal to the ratio $K_K = K_{DT}/ K_{DR}$.

Table 3. The calculation of the increase in the contrast of bone fragments.

Object	Triangular 4,5x5,5 mm	Rectangular 6x5mm	Rectangular 4,5x3,5 mm
K_{DR}, %	4,0	1,8	3,7
K_{DT}, %	36	15	22
K_K	9.0	8.3	6.0

Thus, according to the measurement results, it was found (**Table 3**), that the contrast of images of test objects of medium size made of cortical bone in the digital tomosynthesis image (**Figure 11 e-f**) increases in comparison with the contrast of test objects in the x-ray image (**Figure10 a, b**) in 6, 8.3 and 9 times.

The presence of high-contrast details on the **EqueTom™** digital tomosynthesis images allows for better measurements of spatial dimensions in terms of plan and depth.

To measure the spatial dimensions of the parts, use the “Distance” window (**Figure 9**). When measuring, place the cursor on the extreme points of the measured area and press the buttons to perform the operation.

For the depth measurement, one should find the layers of the beginning of N_b and the end of N_e of a clear observation of the object. The difference of the numbers of layers multiplied by the pinch of the layers:

$$Z_{obj} = (N_e - N_b) \times h$$

The result of multiplication will give Z_{obj} - the size of the object in depth.

It should be noted that when measuring on the tomographic layer, there are no errors of geometrical magnification of the image of an object (Figure 3). Thus, when measuring the size of parts of an object on tomographic layers, the accuracy increases for layer 20 by 13%, and for layer 100 - by 16% compared with measurements on the DR X-ray image.

1.7 Observation of destruction and anomalies of trabecular bone, deviations contrast measurements.

There are many cases when an object is analyzed for the destruction and anomalies of the trabecular bone. The high contrast of the structures of the image characterizing trabecular bones increases the effectiveness of such observations. In the tomographic layers, the trabecular bones are characterized not only by the average X-ray density (brightness) “medium”, but also by the intensity of the deviation of the X-ray density (image brightness) of the trabecular bone elements from the mean value - “sigma”.

In the analysis of DR X-ray images, the measurement of the average X-ray density “medium” (image brightness) is rarely used due to large errors in such measurements. Errors may exceed 100%. Moreover, the “sigma” measurement is not carried out since, due to the overlap of all layers of the object being examined, the results of the “sigma” measurement are difficult to compare with a given survey object.

When analyzing images of CT scanners, the average value of “medium” x-ray density is often measured. As the unit of x-ray density, use Hounsfield (HU). The value of the X-ray density of air in HU is assumed to be “-1000”, and the value of the X-ray density of water in HU is defined as “0”. X-ray density of other objects is calculated relative to water and air. Such calculations for cortical bones give $HU_B > 1000$. The specific value of the x-ray density will depend on the mineral composition of the bone. Mainly from the density of calcium (Ca). This gives the basis for the measured value of X-ray density to judge the development of bone pathologies associated with the loss of mineral density.

CT scanners usually have low spatial resolution, therefore, observation of small bone structures from tomographic images of CT scanners typically is not done and the “sigma” measurement is not performed.

Systems with digital tomosynthesis have several features for measuring the parameters of both cortical and trabecular bones. Usually, the average X-ray density measurement “medium” in the Hounsfield is not carried out due to the lack of methods for considering the influence of the density (brightness) of the adjacent layers.

At the same time, “medium” measurements on tomosynthesis layers can be successfully applied in many practical cases, for example, in identifying bone areas with anomalous mineral density.

To measure the “medium” parameter on the interface (**Figure 6**) on the left below the inscription “MEASUREMENTS”, select the round or rectangular shape of the measurement site and mark it with the cursor. Then, on the selected image of the layer, the measurement area is marked and the value “medium” is read below the inscription “MEASUREMENTS”.

The advantage of the EqueTom™ tomosynthesis system is the high spatial resolution both in the X-ray mode - up to 5 lp/mm and in the tomosynthesis mode - up to 2.2 lp/mm. This makes it possible to measure the “sigma” for the trabecular bone on the tomosynthesis layers.

To measure the “sigma” parameter on the interface (Figure 6) on the left below the inscription “MEASUREMENTS”, select the round or rectangular shape of the measurement site and mark it with the cursor. Then, on the selected image of the layer, the measurement area is marked and the value of “sigma” is read below the inscription “MEASUREMENTS”. The ratio of the “sigma” σ_i values - the intensity of the deviation of the X-ray density of the elements of an object from the average value and the “medium” B_m - average brightness over the measurement site is called the deviations contrast

$$K\sigma = \sigma_i / B_m .$$

The deviations contrast characterizes the relative intensity of small structures in the image of the analysis zone. The results of measurements of the deviations contrast for typical objects on the phantom tomosynthesis layers are shown in **Table 4**.

Table 4. Results of measurement of deviations contrast of typical objects.

Layer number	Description of the object	“medium”, GS	“sigma”, GS	Deviations contrast
10	Phantom zone without bone (soft tissue imitation)	606	26	0.043
10	Small trabecular bone	1150	86	0.075
40	Large trabecular	1090	177	0.16
40	Cortical small-structured bone (osteosclerosis imitation)	1835	80	0.044
60	Loss of trabecular bone (osteoporosis imitation)	1411	51	0.036
70	Cortical bone	1615	70	0.043

Comparison of the results of measuring the deviations contrast shows that the smallest contrast of deviations Kσ = 0.036 was measured in the area of the test hole in the trabecular phantom bone, where the bone tissue was mechanically removed. In the zone of the presence of small trabecular bone, the deviations contrast increases to Kσ = 0.075. In the zone of large trabecular the deviations contrast is doubled Kσ = 0.16. Transformation of the bone structure is characteristic of the destruction of the trabecular bone. In the latter two cases, the measured average X-ray density “medium” is practically unchanged.

The small value of the deviations contrast Kσ =0.043...0.044 according to the results of measurements on the phantom corresponds to a cortical bone and a dense small-structured bone. In the latter case, osteosclerosis may be suspected.

The results of **Table 4** are not supported by significant statistical material and they are only illustrative. At the same time, they clearly show the possibility of using the simultaneous measurement of “medium” and “sigma” in order to diagnose the pathologies of cortical and trabecular bones.

1.8 Artifacts on Images

1.8.1 Shadows on images from adjacent layers.

This type of artifacts is formed due to the limited scanning angle and is present in all diagnostic systems that use the tomosynthesis mode. On-screen picture contains clear sharp focused image of the active tomosynthesis layer plus blurred shadows of adjacent layers.

Image of the active layer can easily be distinguished from the shadows. Image regions with sharp focused small details belong to the active layer, and blurred regions are the shadows from adjacent layers.

By sequential layer pictures scrolling the tomosynthesis system operator implements in-depth focusing of the imaged object.

For example, layer from picture in **Figure12 a** contains sharp images of a splint and osteophytes, whereas layer from picture in **Figure 12 b** contains sharp image of sesamoids.

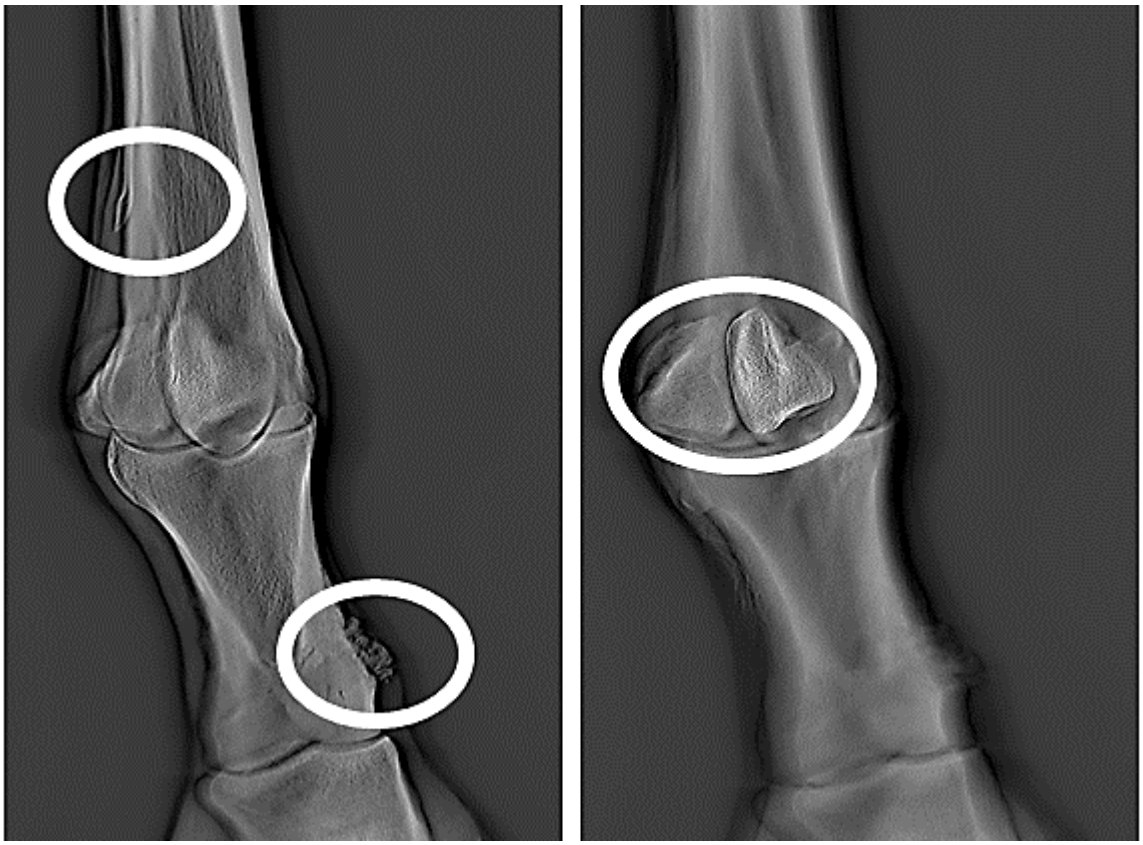

a) b)

Figure 12. LF Foot MDPLO 78 kV. Ovals show sharp images of osteophytes and splint, which are in active layer 102 (a). Another oval shows layer with sharp sesamoids, active layer 44 (b). Distance between layers in depth – 35 mm

This type of artifacts is also called ghost artifacts.

1.8.2 Artifacts due to the animal movement.

Horse (or other animal) should stay motionless during the whole scan process; otherwise, tomosynthesis layers will have motion artifacts.

Figure 13 a shows projection images of a horse foot. The foot movement can be recognized. **Figure 13 b** shows reconstructed tomosynthesis layer for this case. Multiple additional contours are observed, with increased noise, the whole image is unclear.

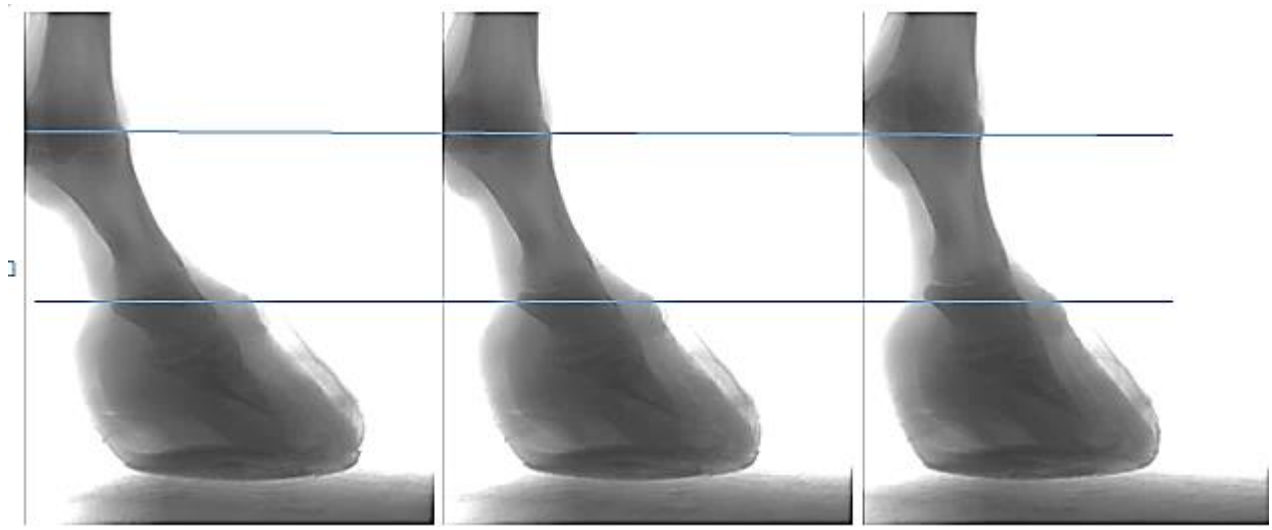

a)

b)

Figure 13. Artifacts due to the horse movement: projections (a), tomosynthesis layer (b).

To eliminate artifacts from motion, you must repeat tomosynthesis scan once you noticed movement of the imaged region.

1.8.3 Image contouring and edges artifacts.

Image contouring artifacts are formed (**Figure 14 a**) at the boundaries of objects in the presence of strong differences in X-ray density. For example, the image regions directly neighboring the bright edge have extra darkness looking like a contour. This type of artifact is not specific to just tomosynthesis systems. On the contrary, it is typical (**Figure 2**) for images of most radiographic and tomographic systems.

Contouring artifacts can be weakened when choosing image processing algorithms with a reduced degree of highlighting or underlining the fine details of images. These artifacts are also called reconstruction artifacts.

The edges artifacts take part if the object is larger then tomosynthesis volume and its edges not present in every X-ray projection. Typically, edges artifacts (**Figure 14 b**) locate on the left and right edges of tomosynthesis images. These artifacts are sometimes called truncation artifacts.

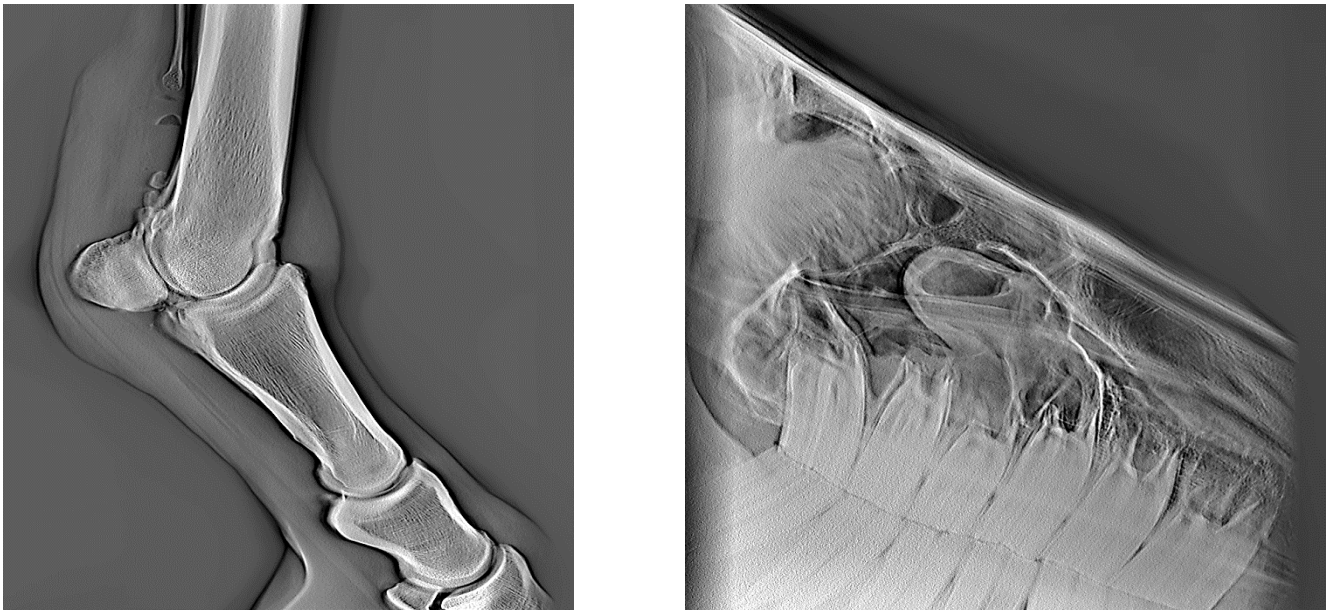

a) b)

Figure 14. Image contouring (a) and edges (b) artifacts.

That location of the edge artifacts on tomosynthesis images is easily recognized by a trained operator.

2 Clinical cases

2.1 Foot (C0007, 27 Feb 2019)

The jumping mare, 6 years old, lameness of the left forelimb observed for 1.5 years. Diagnostic block of the coffin joint of the left forelimb was positive. The EqueTom system was used to examine the phalanges of both forelimbs **(Figure C7.1).**

a)

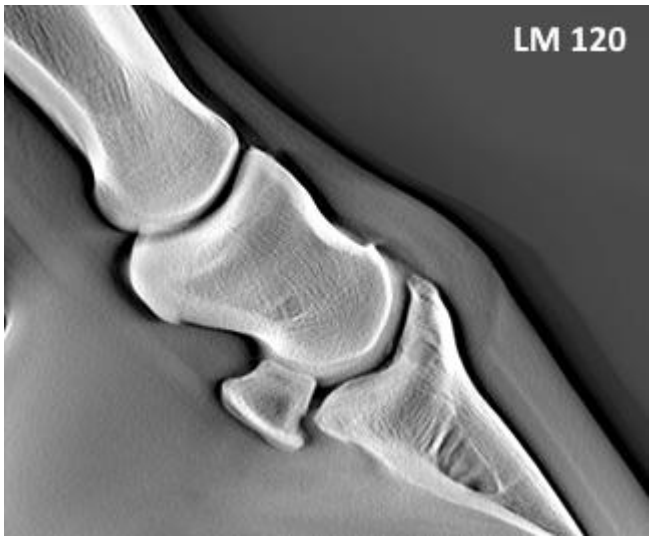

b)

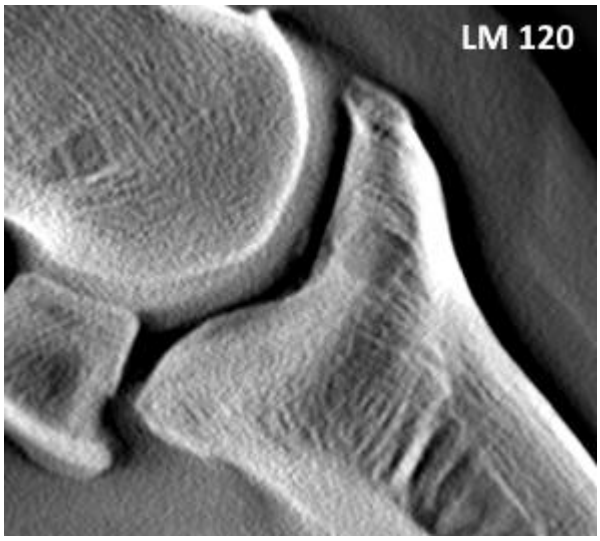

c)

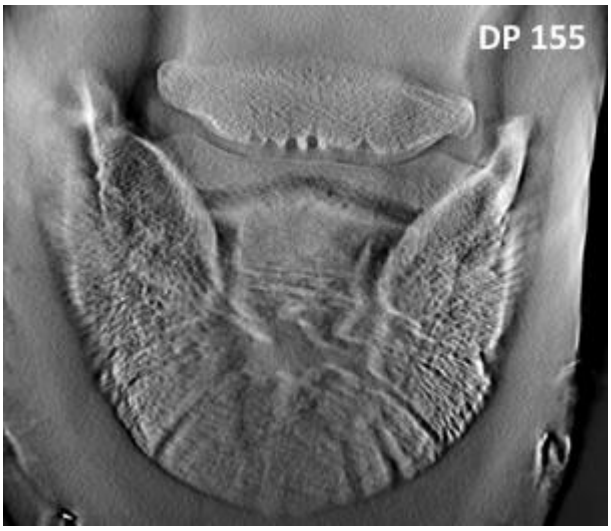

d)

e)

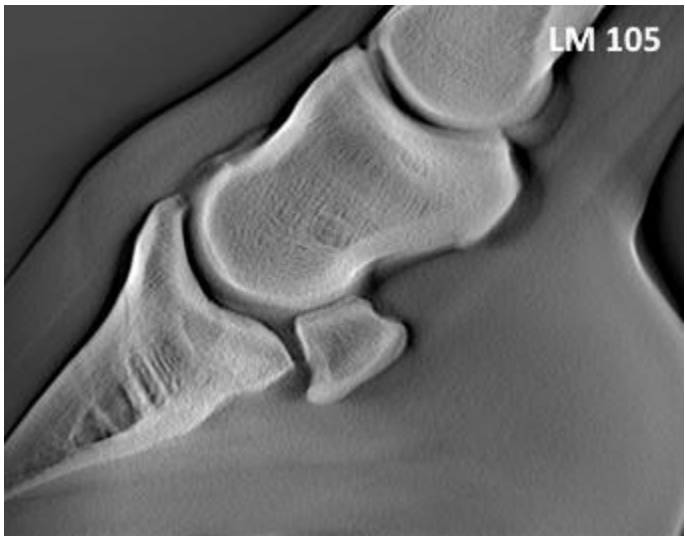

f)

g)

Figure C7.1. Images of tomosynthesis slices of the right **(a,b,c,d)** and left **(e,f,g)** phalanx of both forelimbs in focus on pathology regions.

Comment: Dorsoproximal-palmarodistal oblique view of right forelimb in focus on the extensor process of third phalanx, showing round lucent zone located centrally with small sclerotic margin surrounds the area of radiolucency and irregularity of the articular surface with an isolated fragment nearby **(Figure C7.1 a).**

Lateromedial view of the right forelimb, showing lucent zone located dorsoproximal third phalanx appears to extend to the articular surface of the bone and the isolated fragment near the articular surface of the middle phalanx **(Figure C7.1 b, c).**

Dorsoproximal-palmarodistal oblique view in focus on the middle part of third phalanx, showing round lucent zone with big sclerotic margin surrounds the lucent zone **(Figure C7.1 e).**

Lateromedial view of the left forelimb, showing lucent zone located proximally third phalanx appears to extend to the articular surface of the bone **(Figure C7.1 f).**

Dorsoproximal-palmarodistal oblique view of both forelimbs in focus on the navicular bones, showing increased size and number of trophic channels of these bones **(Figure C7.1 d, g).**

Diagnoses: Subchondral bone cyst of the third phalanx, osteochondritis. Navicular disease.

Link to the complete DTS image series can be found here: https://equetom.forumbee.com/t/m27zrh

Note: When diagnosing with the **EqueTom™** system, it is possible not only to subjectively observe images of tomographic layers, but also to perform objective measurements. According to the results of a single scan, it is possible to measure the size of pathologies along all three coordinates, the X-ray density and its heterogeneity. Measurements create an evidence base for diagnosis.

Thus, on the right foot, the radiolucent zone in the DP projection layer 183 has a size of 7.0x4.2 mm and a depth of 10 mm **(Figure C7.1 a).** The zone contrast is K = -0.45, i.e. zone density about two times lower than the bone density. That corresponds to the density of the liquid. Inside the zone, the substance has a small deviation contrast Kσ = 0.07. In a high probability, the zone is filled with a homogeneous liquid.

When measuring the parameters of this zone by LM projection layers **(Figure C7.1 b, c),** for the layer 120 we get the corresponding dimensions of 7.2x5.0x8.5 mm. The zone contrast is K = -0.50, the deviations contrast is Kσ = 0.06. Thus, measurements of the size and the contrasts of the substance of the zone along the DP and LM projections layers are in good agreement. The measurements difference does not exceed 15%.

For the left leg, measurements of parameters of the radiolucent zone over the DP projection layer 154 **(Figure C7.1 e)** give a size of 6.5 × 5.0 x 13 mm. The zone contrast is K = –0.51, the deviations contrast is Kσ = 0.09. Thus, measurements show that the pathologies on both legs are very similar.

2.2 Fetlock (V0005, 05 Feb 2019)

The dressage stallion 16-year-old lameness of left hind leg. Diagnostic block of fetlock joint was positive. Tomosynthesis scan of this fetlock was made in several projections.

The slices visualized in tomosynthesis examination clearly show the multiple periarticular osteophytes, one of which is isolated on the palmar surface of the distal part of the 3rd metacarpal bone **(Figure V5.1).**

a)

b)

c)

d)

e) f)

Figure V5.1. The images of tomosynthesis slices the fetlock joint left hind leg in latero-medial (**a,c,d,e,f**) and plantare-mediale dorso-laterale (**b**) projections.

In tomosynthesis slices degenerative changes of the lateral proximal sesamoid bone, irregularities of its contours and fragments in the distal part are visualized (**Figure V5.2**).

a) b)

Figure V5.2. The images of tomosynthesis slice the fetlock joint left hind leg in palmo-dorsale (**a**) and plantare-mediale dorso-laterale (**b**) projections.

Narrowing of the joint space of the lateral proximal sesamoid and third metacarpal bones (**Figure V5.3).**

Figure V5.3. The image of tomosynthesis slice the fetlock joint left hind leg in lateromedial projections.

Semi-oval shaped lucency distal of splint bones is the air accumulation in joint capsule after the injection of a local anesthetic during diagnostic block that was made 3 days prior to tomosynthesis scanning (**Figure V5.1 a, e; Figure V5.2 a**).

Diagnosis: fetlock arthrosis, sesamoiditis.

2.3 Pastern (A0004, 28 Jan 2019)

Thoroughbred stallion 4 years old lameness left front leg. Pastern joint was enlarged and painful. The tomosynthesis scans of the left front pastern were done.

In tomosynthesis slices periosteal reaction with the formation of periarticular exostosis of the distal part of the proximal phalanx is visualized (**Figure A4.1 a,b**). Changes are more complicated on the lateral side (**Figure A4.1 b** and **Figure A4.2 a,b**).

a) b)

Figure A4.1. The tomosynthesis scans images of the left front pastern in latero-medial **(a)** and dorso-mediale plantare-laterale **(b)** projections.

The increase bone density and the architecture alterations of distal lateral condyle (**Figure A4.2 a,b,c**).

Pastern joint surface of lateral condyle of proximal phalanx is irregular, joint space is narrowed and subchondral changes are visualized in this region (**Figure A4.2 b**).

The oval-shaped subchondral lucent zone in the intercondylar articular fossa of the distal part proximal phalanx is visualized (**Figure A4.2 c**). This can be with low reliability interpreted as subchondral cyst.

a) b)

c)

Figure A4.2. The tomosynthesis scans images of the left front pastern in dorso-palmar **(a,b,c)** projections.

Diagnosis: arthrosis, osteochondropathy of the pastern joint.

2.4 Head (B0006, 13 Feb 2019)

Gelding 9 years old with purulent excretions from the left nostril, periodically observed during 1,5 years. Tomosynthesis scans of maxillary sinuses and cheek teeth of the horse were done.

In tomosynthesis slices a round-shaped region is observed with diameter about 35 mm with increased intensity in the left maxillary sinus cavity (**Figure B6.1 a,b**).

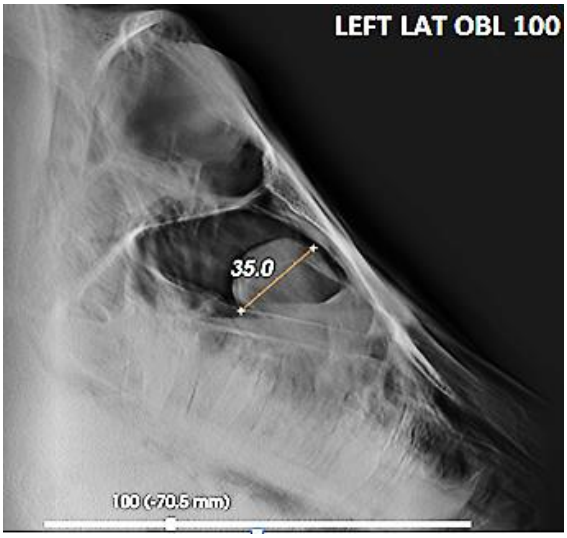

a)

b)

Figure B6.1. The images of tomosynthesis slice the left maxillary sinus and cheek teeth in lateral oblique **(a)** and lateral **(b)** projections.

The same formation in the cavity of the right maxillary sinus was not observed on the Right Lateral or Right Lateral Oblique tomosynthesis slices (**Figure B6.2 a,b**).

a)

b)

Figure B6.2. The images of tomosynthesis slice the right maxillary sinus and cheek teeth in lateral oblique **(a)** and lateral **(b)** projections.

Diagnosis: cyst in the left maxillary sinus.